Meas. Sci. Technol. **9** (1998) 585–591. Printed in the UK PII: S0957-0233(98)88985-6

A multiwavelength daytime photometer—a new tool for the investigation of atmospheric processes

R Sridharan, N K Modi, D Pallam Raju, R Narayanan, Tarun K Pant, Alok Taori and D Chakrabarty

Physical Research Laboratory, Amedabad 380 009, India

Received 4 November 1997, accepted for publication 6 January 1998

Abstract. Technological innovations in optics in the form of a spiral mask system and in electronics in the form of on-line gate scanning of Fabry–Pérot fringes and critical balancing of gate widths for complete background rejection have allowed unambiguous detection of faint dayglow emission features of multiple wavelengths buried in the bright daytime background continuum. The technical details of this unique multiwavelength daytime photometer (MWDPM) and its performance characteristics together with its potential application for the investigation of several geophysical phenomena are presented and discussed.

1. Introduction

The atmospheric airglow and auroral emissions which are the end products of a variety of processes have conventionally been used as tracers of the chemistry and dynamics of the emitting regions. Though the aeronomic processes continue to occur irrespective of the time of the day, these measurements until recently were restricted only to the moonless periods of night-time clear sky conditions. Recent innovations allowed one to overcome these limitations and continuous measurements of faint line emissions in the presence of bright background continuum could be made. These developments now have become a new tool for the investigation of the interaction of complex atmospheric processes. Narayanan *et al* (1989) described a method by which faint line emissions could be unambiguously detected in the presence of a bright background continuum and even line intensities as small as 0.5% of the background could be measured. Since its development this instrument had been undergoing significant improvements and the present level of detection had been brought down to better than 0.05% of the background intensity (Sridharan *et al* 1992a). This task has been accomplished by means of a critically maintained optical system consisting of a temperature-tuned narrowband (3 Å) interference filter, a pressure-tuned Fabry–Pérot (FP) etalon (FSR 4 Å), a chopping mask assembly which alternates between two regions in the FP fringe plane (typically separated by 0.7 Å) and two adjustable gated photon counters which are synchronized to the above referred regions. Under tuned conditions of the FP etalon one of the regions (usually the central one) contains the emission feature together with the background while the (outer) annular region contains only the background contribution at a wavelength whose centre is separated by just 0.7 Å. With the FP etalon pressure tuned to the emission line and with an overall spectral resolution of $\leq 10^4$ the difference in photon counts from the two independent counters, obtained after a selectable integration time, represents the emission line intensity. This method has been shown to overcome all the limitations of the earlier attempts at dayglow photometry (Noxon and Goody 1962, Bens *et al* 1965) and has very successfully been used in the detection of O I 6300 Å airglow emission during daytime conditions. However, it should be noted that pioneering contributions have been made in the field of high-resolution spectrometry for line profile determination by Roesler and his group in Wisconsin, USA, and Jacka and his group in Australia (Roesler and Mack 1967, Barmore 1977, Cocks and Jacka 1978). Because the present development is a photometer, no further technical details on the multi-etalon spectrometers are provided in this paper. The presentation and discussion revolve around photometeric observations only.

Several new results pertaining to the relative importance of the processes responsible for the O I 6300 Å dayglow and to geophysical features like the development of the equatorial ionization anomaly (EIA) and equatorial spread *F* (ESF) have been obtained and reported in the literature (Sridharan *et al* 1992b, 1994, Pallam Raju *et al* 1996).

0957-0233/98/040585+07$19.50

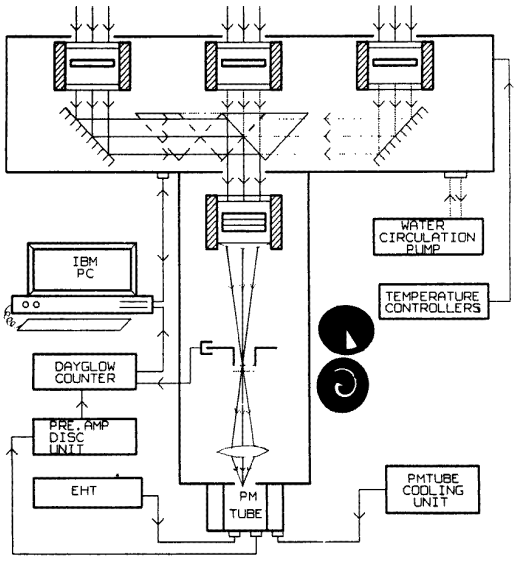

Figure 1. A schematic diagram of the multiwavelength daytime photometer (MWDPM).

The dayglow photometer (DGP) which is routinely operated now, has a limitation of being able to monitor only one wavelength at a time. A change of monitoring wavelength involves changing the interference filter and also altering the tuning conditions (usually pressure) of the FP etalon. This is cumbersome when nearly simultaneous measurements of more than one wavelength are needed. Such a need arises in the investigation of large-scale atmospheric dynamics and also of the processes associated with the daytime auroral emissions. The more the wavelengths to be monitored the more difficult it becomes to change the tuning conditions. In order to overcome the above difficulties and allow the photometer to detect different wavelengths nearly simultaneously, Sridharan *et al* (1993) suggested a novel mask design for multiwavelength dayglow photometry. The proposed mask design made use of the spatial separation of the various wavelengths under consideration by the FP etalon. A new daytime photometer incorporating several innovations, both in the optics (employing the spiral mask design proposed by Sridharan *et al* (1993)) and in the electronics, has successfully been developed from the conceptual stage and had been used for the first-ever systematic ground-based measurements of (i) the daytime auroral emissions from the Indian station in Antarctica (Pallam Raju *et al* 1995) and (ii) the various daytime line emissions from the mesospheric–thermospheric regions from low latitudes. The following sections describe the salient features of the multiwavelength daytime photometer (MWDPM) and some of the sample results both from the high- and from the low-latitude regions.

2. Instrument details

A schematic diagram of the MWDPM is shown in figure 1. The optics is contained in two units. The first compartment on top contains the narrow-band interference filters. At present it is designed to hold three of them. These interference filters are housed in separate housing enclosures which are independently maintained at appropriate temperatures to within $\pm 1\,^{\circ}$C using Peltier elements and bipolar temperature controllers. The filters are thermally isolated and the tuning temperature is determined for the actual instrumental orientation taking into account the mutual tilting of the mechanical and optical axes, if any. A coolant pump circulates water through small brass tanks which are in thermal contact with the other side of the thermoelectric Peltier elements. This arrangement essentially serves as a heat sink when the filter is being cooled. In the filter box, right below the filters at the left- and right-hand extremes, front-silvered mirrors are fixed at an angle of 45° in order to deflect the incident light beam at right angles. In between these two mirrors a right-angled prism with both the faces front silvered is mounted on a rail. One face of the prism and one of the mirrors forms a 'periscopic combination' and, depending upon the position of the prism, light from filter 1 or 3 could be directed into the following optics. At the right-hand extreme position of the prism light passing through the extreme left filter (F1) is let through into the hind optics. At the middle position of the prism light from the extreme right-hand filter (F3) is selected and at the far end of the prism the central filter (F2) is chosen. The actual position of the right angle prism is precisely determined, being sensed by means of an opto-coupler and the periodical, programmed, movement is accomplished by means of a stepper motor controlled by a personal computer. The control sequence will be discussed later.

The light that comes through the filter unit is now allowed to pass through a Fabry–Pérot etalon. Bearing in mind the large wavelength range, which covers the whole of the visible spectrum, a specially coated Fabry–Pérot etalon has been used. In this case the etalon is coated for a flat response in the range 3900–8000 Å with reflectivity in the range 85–90%. The optically contacted FP etalon has an airgap of 200 μm with a clear aperture of 20 mm and was procured from Melles Griot Ltd. The etalon is housed in a small pressure-tight chamber allowing pressure tuning of the same. Furthermore, selection of the wavelengths is accomplished by electronic gate scanning/delay techniques to be discussed later. A camera lens that follows the FP etalon forms concentric fringes at the image plane.

3. The novel mask assembly

In the earlier version of the single-wavelength dayglow photometer the masks had two well defined annular zones separated by about 0.7 Å with a free spectral range (FSR) of about 4 Å at 6300 Å. In the new mask design these discrete zones are replaced by a zone that continuously spirals outwards from the centre (see the inset in figure 1). Care is taken to account for the $1/r^2$ dependence of the fringe diameters by proportionately reducing the width of the spiral while radially moving outwards. The wavelength span of the spiral is at least up to one FSR of the longest wavelength to be measured. Thus any spectral element within the pass band of the etalon has at least one of its

fringes within the span of the spiral mask. The spiral mask is followed by a rotor mask, mounted concentrically with respect to the former and kept very close to it. The rotor mask has a 30° transparent wedge that extends to the outermost diameter of the spiral (see the inset in figure 1). As the rotor mask rotates, the 30° opaque wedge in the spiral provides a complete blank once during every rotation and the interception of this null zone acts as a source for the generation of a reference signal. A reference slot with a small cut-out and an opto-coupler mounted to match the cut-out are aligned with the null zone. With this arrangement, the rotation of the rotor would periodically provide reference pulses that would in turn coincide with the beginning of the innermost region of the spiral. With the static spiral mask intersecting a portion of the circular fringes, the maximum signal is obtained when the rotor position completely overlaps the intercepting region. Since the rotor rotates at a constant speed with respect to the opto-coupler, the emission feature appears at a constant time interval. Thus the *spatially* displaced fringes of various wavelengths would be seen as *temporally* separated ones. By appropriately gating the photomultiplier and linking it to the choice of filters at the front end, different emission features could be detected and measured. In the present design, unlike the single-wavelength DGP, no definite region is earmarked for the so-called background continuum. However, since the emission feature extends to only a 30° segment of the spiral, the adjoining region itself could conveniently be taken to represent the background contribution which would be centred at a wavelength just separated by (1 Å) namely, approximately one tenth of the FSR corresponding to the longest wavelength of interest. The width of the gating pulses could be adjusted for perfect background rejection for white light illumination. Change of filters is accomplished with the help of a personal computer by means of menu-driven, in-house-developed software. The gate delays and widths are also generated and controlled by the same computer. Further details of the conceptual design of the mask have been highlighted by Sridharan *et al* (1993). The above concept of the mask, realized using computer-aided design, has successfully been implemented in the MWDPM.

Once the emission feature has been selected by the pre-filter and appropriately gated by the FP etalon and mask combination, it is re-imaged on to a photomultiplier (S-20 EMI 9863A) tube which is thermoelectrically cooled. After proper signal conditioning the pulses which are ECL compatible are converted to TTL compatible ones and fed as inputs to the synchronously gated photon counters. One of the counters is locked to the signal domain and the other to the background domain. After integration to a pre-set time, typically 10–20 s, the difference in counts is obtained and plotted on line. This difference in counts represents the emission line intensity.

In actual operation all the events discussed above have to be executed sequentially. To start with, a mirror (not shown in figure 1) mounted above the filter unit allows the selection of different elevations (look angles) of the sky. The mirror elevation is altered sequentially in order to scan the region of emission spatially. For every elevation angle of the mirror, the filters are sequentially selected. On the selection of a filter, an appropriate gate delay for that wavelength is introduced and the photomultiplier-gated photon counters are activated for a duration for appropriate background rejection. The method of determining the gate delays and widths is dealt with in the next section. Data corresponding to one particular wavelength, namely the difference between the two counters, are plotted with time, on line, by the computer system. After this, the stepper motor is moved to the second filter and this sequence is repeated. After the whole sequence for all the three filters has been completed, the mirror elevation is changed to a new direction and the whole cycle is repeated for that direction. Usually the lowest elevation that one could attain is about 10° in the sky and this strongly depends on the viewing conditions. The various elevations are pre-programmed and the instrument is fully automatic after its initial setting.

4. Active electronic gate scanning

Typically the Fabry–Pérot fringe systems are scanned by (i) changing either pressure or temperature, which essentially means varying the path length owing to the change in the refractive index, (ii) varying the gap between the plates of the FP etalon, which amounts to changing the optical path mechanically, and (iii) changing the angle of incidence. In the case of interferograms being available, radial scanning of the fringes can be carried out off line, which could be linearized later. The present technique (incorporated in the MWDPM) which employs a combination of the FP etalon and the spiral mask together with synchronously gated photon counters, has made available a novel method of electronically scanning the FP fringes ‘on line’. This is in addition to the available standard methods of scanning mentioned above. In this new method, none of the FP-related parameters are changed and the technique is as follows.

The gate pulses corresponding to two wavelength intervals centred at λ and $\lambda + \partial\lambda$ are triggered by means of a chopper-generated reference pulse and the initial time delay provided by the clock pulses of the PC is incremented in hundreds of microseconds, the smallest increment possible being in units of microseconds. It amounts to ‘dual gate scanning’, the gates corresponding to ‘signal plus background’ and only ‘background’ are being scanned simultaneously and synchronously. The difference in photon counts corresponding to these two gates is monitored ‘on line’. Because one gate delay matches with the time (the position of the fringe) when the emission feature cuts through there would be a build up of intensity. When the gate leaves this region, in the time domain, the intensity falls and when the second gate sweeps through the same region the difference would give negative counts. Perfect instrumental scans could be obtained using this method. The gate widths could be adjusted for obtaining symmetrical profiles (both positive and negative amplitudes) and also for complete rejection of the background. One of the typical instrument scans for a He–Ne laser is depicted in figure 2. When the

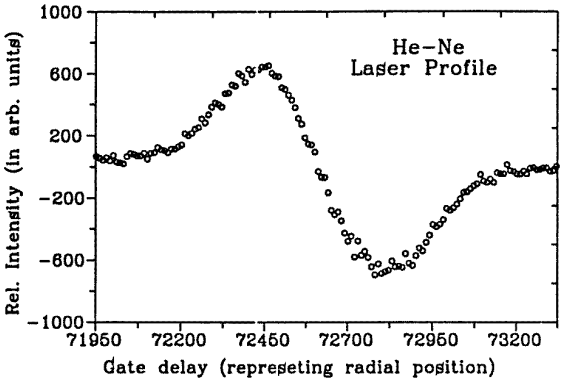

Figure 2. The relative intensity of the laser beam obtained with the dual gate scanning.

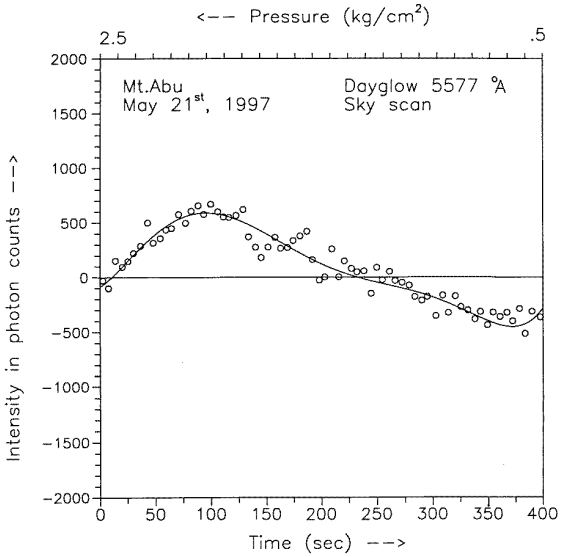

Figure 3. A typical pressure scan of the day sky and the differential profile of O^1S 5577 Å dayglow with 1 s integration of the datum point.

filter bandwidth is considerably narrower than the free spectral range (FSR) of the FP etalon, the filter pass band characteristic would modulate the signal intensities. In order to overcome this effect, the signal and background gates are positioned at the maximum transmission of the filter and adjacent to it. Appropriate correction is made by gate-width adjustment; that is, the excess intensity (say signal) through one of the gates is compensated by a longer duration gate width (background). Once the preliminary gate settings have been done, the system is made to look at the daytime sky and a pressure scan taken. Depending upon the signal intensity, a well defined differential profile is obtained. The gate widths and delays are further trimmed to obtain a symmetrical pressure scan (figure 3) similar to the one depicted for a laboratory spectral source. After one has ensured these settings the FP etalon pressure is kept fixed at the positive peak (usually) of the profile before it is put into data-collection mode.

5. Constraints, performance evaluation and discussion

Before the performance of the new multiwavelength daytime photometer is presented the constraints under which it has to function are, briefly discussed. Typically the dayglow intensity could be of the order of 5–10 kR (it could even be more over the belt of the equatorial ionization anomaly for the thermospheric emissions) with the background intensity being of the order of 10 MR $Å^{-1}$. The continuum background has added complexities in the form of Fraunhofer absorption features in addition to the telluric absorption lines and the ring-effect emission from the terrestrial atmospheric constituents. Furthermore, the background is partially polarized. The finer absorption features, if any are present, would no doubt be seen in the spectrum at high resolutions, as had been discussed by Roesler and Mack (1967), Barmore (1977) and Cocks and Jacka (1978). However, in the region of 6300 Å of the solar spectrum, it had been shown by Barmore (1977) that no noticeable atmospheric absorption lines were present. This aspect, added to the ring effect which tends to fill the absorption bands, if there are any (Barmore 1975), would tend to smooth out the continuum in this wavelength band. Furthermore, in the present application of dayglow photometry, unlike the dayglow spectrometry attempted by the earlier workers, the spectral window is typically 0.5–0.7 Å and the field of view of the instrument is about 4°. These two aspects integrate the emission feature both spectrally and spatially and would eventually smooth out the finer structures to a still greater extent, while retaining the identity of the emission feature to a reasonably good extent. The choice of the spectral width of 0.7 Å had been independently found to be appropriate through a study of the solar spectrum by means of a McPherson grating monochromator (type 207, 0.67 m scanning monochromator) operated at a maximum resolution of $\simeq$1 Å centred around the wavelength of interest (5577 ± 5 Å). The smoothing out of the absorption features could clearly be seen during such medium-resolution studies. The validity of the above statement is demonstrated below. Figure 3 depicts the typical dayglow pressure scan, after one has optimized the gate delays and widths; this time it is O^1S 5577 Å emission. In spite of the integration period being just 1 s, the differential emission profile is seen to come out very clearly. Now, keeping the rest of the instrumental parameters the same, sunlight is directly reflected into the system. Care is taken not to saturate the photomultiplier tube by appropriately diffusing the reflected light at the entry port of the photometer. This ensures that light from all parts of the solar disc is given equal weighting, as for light scattered from the atmosphere. The method, in principle, is similar to the one discussed by Barmore (1975). A repeat of the pressure scan is taken now and the result is depicted in figure 4. One could clearly see that the finer spectral features of the solar spectrum had been completely integrated out and the pressure scan yields a nearly flat profile. It should be noted that the sky scan and the solar scan were performed within a 10 min time

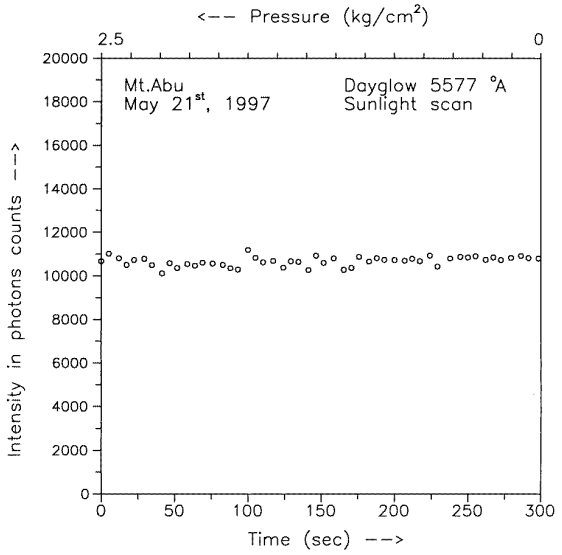

Figure 4. A pressure scan of the direct solar spectrum in differential scanning mode.

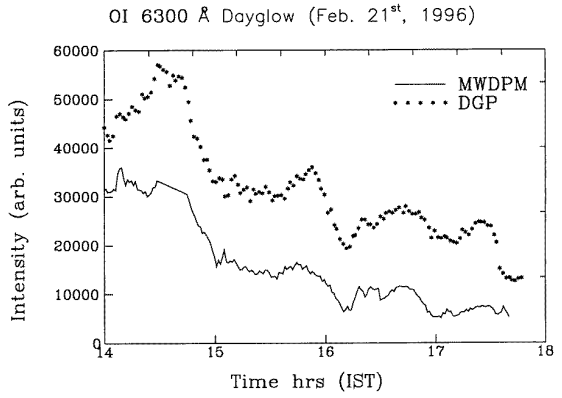

Figure 5. The similar variation of O I 6300 Å dayglow intensity seen both by the MWDPM and by the DGP, validating the performance of the MWDPM.

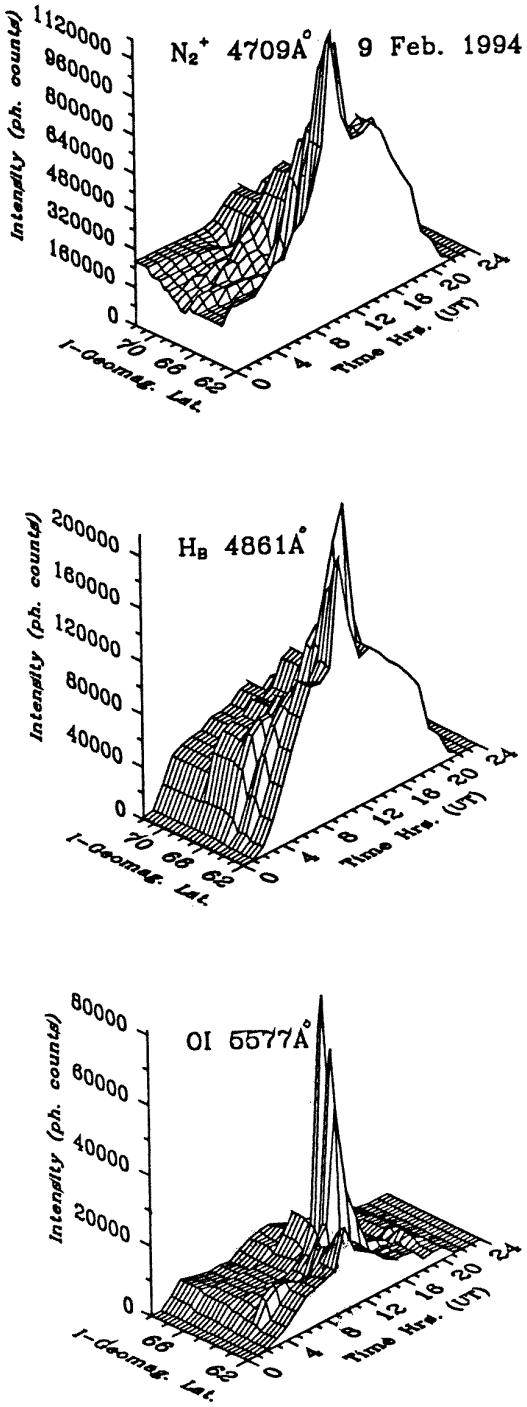

Figure 6. Observations of auroral emissions at 4709, 4861 and 5577 Å from Antarctica.

interval under identical instrumental operating conditions. This has also been verified at different times of the day. The second aspect is the partially polarized nature of the sky background while the dayglow is unpolarized. If the background contribution is totally removed, the resultant dayglow intensity should not be modulated with the rotation of a polarizer at the entrance aperture. This indeed had been found to be so, thus validating the method of dayglow detection. All these tests were performed along similar lines to the single-wavelength DGP discussed in the literature (Narayanan *et al* 1989) and were carried out at the Optical Aeronomy Laboratory at Mount Abu, India.

In this context, it should also be noted that 'high-resolution' line profile measurements continue to be extremely difficult due to the presence of absorption features on the one hand and due to the very narrow 'FOV' and associated small volume of emission and also the extremely narrow spectral window one considers at any instant (typically two orders of magnitude smaller than the line width itself) on the other. As a consequence, as is well known, due to Jacquinot's criterion which demands that the product of luminosity and resolution be a constant for any instrument type, the SNR is extremely low and one has to seek recourse to very-long-time integration. This is the reason for the complexities involved in the field of high-resolution spectrometry (Cocks and Jacka 1978, Barmore

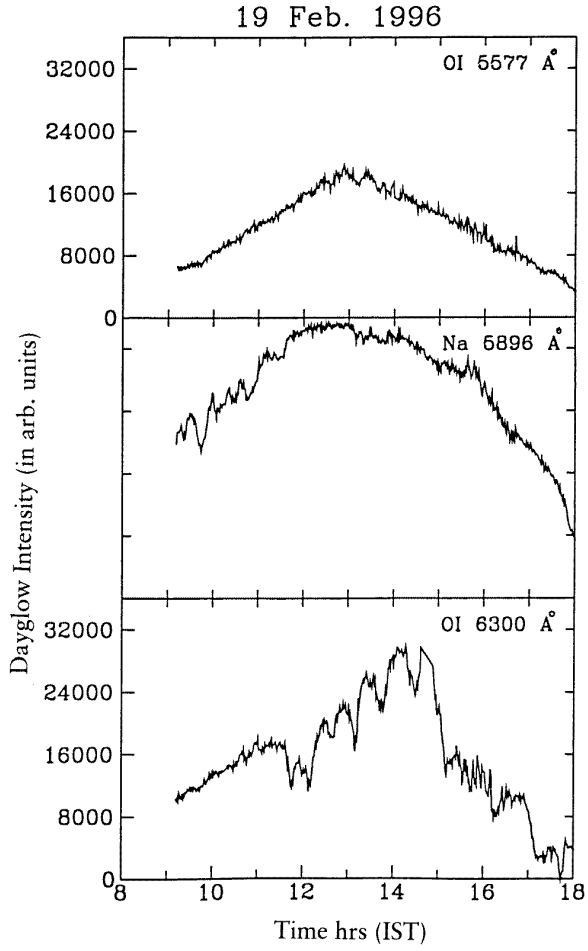

Figure 7. Observations of 5577, 5896 and 6300 Å dayglow emissions from low latitudes.

1977). However, as discussed above, in the present case, photometric detection and measurements do not face these added constraints.

Both the presently described MWDPM and the first version of the dayglow photometer (DGP) are relative-intensity-measuring instruments, insofar as the gate-width adjustment, which is one of the instrumental settings for background removal, is typically worked out only once and for all (it is done manually, which is subjective), with periodical checks once every few days. The variation in the background part during the course of the day is taken into account, within the spectral interval of about 1 Å near and around the emission feature, because it varies by the same amount and the subtraction procedure takes care of it. Absolute calibration is rather involved. However, one could note that the purpose of building an instrument which could reveal the day-to-day variabilities and also those during the course of the day in dayglow has been shown to be satisfied by its successful application to thermospheric processes.

The MWDPM was first put on a trial run in a single-wavelength mode of operation together with the standard dayglow photometer operating on O I 6300 Å airglow emission line originating from about 200 km altitude. Figure 5 shows the actual data obtained from both the instruments. Nearly identical variations are recorded in both the instruments. The absolute intensities are not expected to be equal insofar as both of them are uncalibrated, as mentioned above. One of the interesting observations is that the data scatter for the MWDPM is significantly less than that for the DGP, which is ascribed to the improved mask fabrication methods adopted in the former. The minimum detection limit is comparable to that of the DGP and is $<0.1\%$ of the background.

The first field trial on MWDPM was conducted from Maitri (70.7 °S, 11.6 °E; 62.8 °I geomagnetic latitude), the Indian station in Antarctica, and 'systematic and continuous' measurements of daytime auroral emissions at 3914, 4278, 4709, 4861, 5577 and 6300 Å were made. Figure 6 shows the typical results obtained from this exploratory campaign which identifies regions of energetic particle precipitation in and around Maitri. Owing to the nearly simultaneous measurements at various wavelengths, it was possible to infer the relative importance of the energetic particles (electrons or protons) that give rise to a particular auroral event during varying geomagnetic activity (Pallam Raju *et al* 1995). Measurements from a low-latitude region, namely from Mount Abu (24.61 °N, 73.73 °E; 19.2 °N dip latitude) are currently being made on a routine basis on airglow emissions originating from lower and upper thermospheric regions, namely sodium D lines (5890 and 5896 Å) and oxygen green (5577 Å) and red (6300 Å) lines, to identify vertically propagating wave-like disturbances. Figure 7 depicts typical results from the ongoing study.

The new multiwavelength daytime photometer is considered to be a valuable addition to the existing techniques and is expected to provide important information on the large-scale dynamical processes in the atmospheric regions. Though in the presentation above the orientation is towards the investigations in optical aeronomy, the applications of this technique to other disciplines are left only to the imagination of the user.

Acknowledgments

The help rendered by Mrs Vijaya Mutagi in the fabrication of the necessary control electronics and the help in the fabrication of the instrument by Messrs C L Gajjar and (the late) S M Suthar is duly acknowledged. This work is supported by the Department of Space, Government of India.

References

Barmore F E 1975 *J. Atmos. Sci.* **32** 1489
——1977 *Planet. Space. Sci.* **25** 185
Bens A R, Cogger L L and Shepherd G G 1965 *Planet. Space. Sci.* **13** 551
Cocks T D and Jacka F 1978 *J. Atmos. Terrestr. Phys.* **41** 409
Narayanan R, Desai J N, Modi N K and Sridharan R 1989 *Appl. Opt.* **28** 2138

Noxon J F and Goody R M 1962 *J. Atmos. Sci.* **19** 342
Pallam Raju D, Sridharan R, Gurubaran S and Raghavarao R 1996 *Ann. Geophys.* **14** 238
Pallam Raju D, Sridharan R, Narayanan R, Modi N K, Raghavarao R and Subbaraya B H 1995 *J. Atmos. Terrestr. Phys.* **57** 1591
Roesler F L and Mack J E 1967 *J. Physique* **28** Suppl C2 313
Sridharan R, Haider S A, Gurubaran S, Sekar R and Narayanan R 1992b *J. Geophys. Res.* **97** 13 715
Sridharan R, Narayanan R and Modi N K 1992a *Appl. Opt.* **31** 425
Sridharan R, Narayanan R and Pallam Raju D 1993 *Appl. Opt.* **32** 4178
Sridharan R, Pallam Raju D, Raghavarao R and Ramarao P V S 1994 *Geophys. Res. Lett.* **21** 2797